# Accepted Manuscript

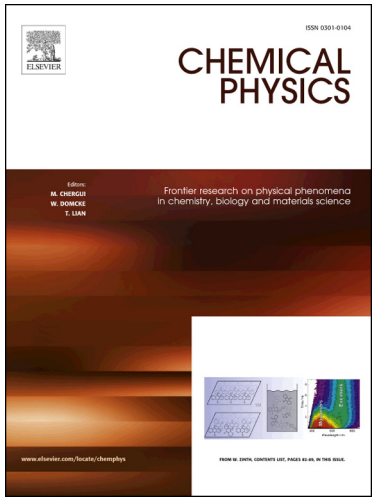


A simulation of free radicals induced oxidation of dopamine in aqueous solution

Branislav Milovanović, Jelica Ilić, Ivana M. Stanković, Milana Popara, Milena Petković, Mihajlo Etinski

PII: S0301-0104(19)30248-4
DOI: https://doi.org/10.1016/j.chemphys.2019.05.001
Reference: CHEMPH 10374

To appear in: *Chemical Physics*

Received Date: 7 March 2019
Accepted Date: 1 May 2019

Please cite this article as: B. Milovanović, J. Ilić, I.M. Stanković, M. Popara, M. Petković, M. Etinski, A simulation of free radicals induced oxidation of dopamine in aqueous solution, *Chemical Physics* (2019), doi: https://doi.org/10.1016/j.chemphys.2019.05.001

# A simulation of free radicals induced oxidation of dopamine in aqueous solution

Branislav Milovanović, Jelica Ilić

*Faculty of Physical Chemistry, University of Belgrade, Studentski trg 12-16 11000 Belgrade, Serbia*

Ivana M. Stanković

*ICTM, University of Belgrade, Njegoševa 12, 11000 Belgrade, Serbia*

Milana Popara, Milena Petković, Mihajlo Etinski

*Faculty of Physical Chemistry, University of Belgrade, Studentski trg 12-16 11000 Belgrade, Serbia*

**Abstract**

Understanding the basic chemistry between highly reactive free radicals and dopamine is an important step in characterizing the antioxidative activity of catecholamine neurotrasmitters. In this work, we simulated the reactions between dopamine and hydroxyl, peroxyl and methoxy radicals in aqueous solution by employing first principle molecular dynamics based on density functional theory and the BLYP functional. The simulations provide mechanistic insight into the reaction mechanisms but underestimate reaction timescales. The failure of the BLYP functional to address the formal hydrogen atom transfer barriers between dopamine and free radicals is attributed to the self-interaction error.

*Keywords:* density functional theory, molecular dynamics, Wannier functions

## 1. Introduction

Oxidative stress is a result of an imbalance in pro-oxidant/antioxidant homeostasis or unregulated production of toxic reactive oxygen species, such as hydrogen peroxide, nitric oxide, superoxide and hydroxyl radicals. These intermediates cause extensive damage to DNA, proteins and lipids and thus they must be somehow conciliated [1, 2]. Organism antioxidant defense involves several different strategies, enzymatic and non-enzymatic, both in lipid and aqueous phase. Reactive radicals are insatiable towards many substances and specific enzymatic scavenging alone would be impossible. Therefore, small molecules add significant contributions to the antioxidant defense already provided by the enzymes superoxide dismutase, catalcase and glutathione peroxidases [2].

Free radicals are blocked by direct addition to antioxidants, electron transfer or formal hydrogen atom abstraction from antioxidants. The hydrogen abstraction mechanism involves a transfer of an electron and proton either simultaneously or individually, one by one. Also, the whole process can be solvent-mediated resulting in a complex reaction. The formal hydrogen atom transfer mechanisms can be classified in two groups: a transfer of a hydrogen atom in a single elementary step and a separate transfer of the proton and the electron, which involves an intermediate formation. The former mechanism includes a hydrogen atom transfer (HAT) when a proton with one of its bonding electrons is transferred, proton-coupled electron transfer (PCET) which includes a transfer of a proton and an electron from a different bond, and multi-site proton-coupled electron transfer (MS-PCET) when the proton and electron are transferred to different molecules. The later mechanism includes the proton-electron sequential transfer (PEST) or the electron-proton sequential transfer (EPST). In addition, when solvent molecules assist the sequential transfer, it can be classified either as the sequential proton-loss electron-transfer (SPLET) or sequential proton-gain electron transfer (SPGET), depending on which particle arrives first to the acceptor.

Figure 1: Chemical structure and atom numbering of dopamine. The amino group is protonated at the physiological pH values.

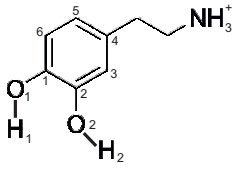


Catecholamines are a class of neurotransmitters which include adrenaline, noradrenaline and dopamine. Beside their physiological role, they exhibit an antioxidant activity since the catechol moiety has favorable redox properties. It is found that neurodegenerative diseases are followed by the changes in catecholamines concentrations [1], which supports the conclusion that these species might respond to the oxidative stress related to neurodegenerative diseases. Various attempts to resolve the

*Email address:* etinski@ffh.bg.ac.rs (Milana Popara, Milena Petković, Mihajlo Etinski)

antioxidant activity of catecholamines and other phenols by employing diverse quantum-chemical and experimental methods provided different reaction mechanisms [3, 4, 5, 6, 7, 8, 9, 10, 11, 12, 13, 14]. Álvarez-Diduk and Galano [8] showed that adrenaline and noradrenaline are efficient in reducing oxidative stress through SPLET in aqueous solution at physiological pH values. Dimić et al. [12] discussed the most probable reaction mechanism towards DPPH radical abstraction by naturally occurring catecholamines combining static density functional calculations with UV/VIS spectroscopy. They also showed that SPLET is the most probable mechanism in polar solvents, while in non-polar solvents there is competition between SPLET and HAT/PCET mechanisms. These authors also investigated antiradical activity of catecholamines towards substituted methylperoxy radicals and they concluded that the most probable mechanisms are HAT and SPLET [6]. In addition, Dimić et al. [15] showed that vanillylmandelic acid, the end-stage metabolite of the catecholamines, exhibited SPLET-like mechanism towards radicals. On the other hand, Iuga et al. [7] argued that the hydroxyl radical scavenging by dopamine in aqueous solution at the physiological pH values proceeds via sequential electron proton transfer, whereas in the lipidic environment the hydrogen atom transfer and radical adduct formation dominate.

Previous computational studies on catecholamines' oxidation examined various reaction steps as independent events by employing continuum models in order to account for the solvent effects [7, 8, 6, 12]. This type of analysis limits the information that can be acquired about the mechanistic bottlenecks of different mechanisms. Besides, water molecules not only do provide hydrogen bonding and electrostatic interaction with the solute but may also act as the proton acceptors. Hence, to overcome these difficulties and provide an insight into catecholamines antioxidation activity, we performed first principle molecular dynamics simulations of dopamine (see Figure 1) in presence of hydroxyl, peroxyl and methoxy radicals solvated with water molecules under periodic conditions. This powerful computational method allowed us to treat solvent molecules on the equal footing with the solute molecules. Since density functional based molecular dynamics is a computationally expensive method, previous studies on radicals and their reactions with organic molecules in the gas phase and aqueous solution [16, 17, 18, 19, 20, 21, 22, 23, 24, 25] employed the functionals based on the generalized gradient approximation (GGA). These studies reported reaction mechanisms of various radicals with nucleobases and small antioxidants. Prompted by these findings, in this work we also used a GGA functional. Our results showed the formal hydrogen transfer from dopamine to free radicals proceeds via a single step process, without the formation of stable intermediate species. On the other hand, the simulation failed to properly account the reaction free energy barriers for these processes due to the self-interaction error present in the employed density functional.

## 2. Computational Details

*Ab initio* molecular dynamics simulations were performed with the CP2K software package [26]. These simulations incorporate electronic structure density functional theory calculations within a classical molecular dynamics scheme. We used the BLYP [27, 28] functional in conjunction with Grimme's D3 correction for dispersion interactions [29]. The pseudopotentials of the GTH type [30] were employed in order to represent core electrons' interactions. Valence orbitals were expanded in a mixed Gaussians and plane waves basis [31]. Converged results were obtained using the finest grid level cutoff and relative cutoff of 330 and 60 Ry, respectively. Target accuracy for the SCF convergence was set to $5.0 \cdot 10^{-7}$ in atomic units. The system was thermalized to 298 K using CSVR thermostat [32]. The equilibriation and production runs were performed under the NVT ensemble and they lasted 2 and 10 ps, respectively. The time step for the numerical integration of the equations of motions was set to 0.5 fs. The trajectories were analysed by using the TRAVIS program package [33].

Dopamine was solvated with 52 water molecules. This is a relatively small number of solvent molecules, but sufficient enough to model the first and a part of the second hydration shell around the solute. The size of the simulation box was determined by the procedure explained elsewhere [34]. The lengths of orthorhombic cell vectors amounted to 11.08, 11.99 and 13.04 Å for $x$, $y$ and $z$ components, respectively. Simulations of the reaction paths for radicals' attacks on dopamine in aqueous solution were performed using different starting configurations in order to avoid bias due to the initial conditions. 21, 3 and 7 reactive trajectories were simulated for hydroxyl, peroxyl and methoxy radicals, respectively. The initial configurations were extracted from the production run. The hydroxyl radical was prepared by removing a hydrogen atom from a randomly selected water molecule, whereas peroxyl and methoxy radicals were prepared by removing two water molecules and inserting corresponding radicals. Time steps for these runs were 0.2 fs, and the simulations were interrupted a few hundreds femtoseconds after a reaction took place. In order to monitor electronic degrees of freedom, we computed Wannier orbitals. These functions are localized on chemical bonds and lone pairs. They are computed by a constrained unitary transformation of the original Kohn-Sham orbitals.

## 3. Results and Discussion

### *3.1. Hydroxyl radical*

We find that the hydroxyl radical attack on dopamine proceeds via PCET or MS-PCET mechanisms depending on the distance between the dopamine and hydroxyl radical. If the hydroxyl radical is in the first solvation shell of the dopamine and positioned close to hydroxyl groups then the reaction mechanism is PCET. Otherwise, dopamine cation is sufficiently acidic to transfer a proton from hydroxyl groups to a water molecule so that the reaction mechanism becomes MS-PCET.

By analyzing the electronic and the nuclear motion along reaction paths, we determined that 16 out of 21 trajectories in

our simulations proceeded via MS-PCET. On the other hand, 5 out of 21 trajectories resulted in PCET mechanism. In both mechanisms we find that the electron is always removed from the $\pi$ orbital of the catechol group with no $\sigma$ electron density being lost neither from the O1-H1 nor the O2-H2 bond. Particularly, the electron leaves the C1 or C2 atoms, depending on which one is closer to the radical, which is also reported by García-Hernández and Garza [35]. Another common property of all reactions is that they always start a few femtoseconds after beginning of the simulations as well as that they are finished within less than one picosecond. This implies that these reactions are barrierless.

Figure 2: Upper panel: Insets with configurations during PCET reaction of dopamine with hydroxyl radical. Other water molecules were omitted for clarity. The WCs are depicted by pink ("$\alpha$" spin - $WC^{\alpha}$) and green ("$\beta$" spin - $WC^{\beta}$) spheres, whereas violet sphere represent $WC^{\beta}$ of moving electron. Middle panel: Evolution of O1-H1 (black line), H1-$O^{\cdot}$ (red line), $WC^{\beta}$-$O^{\cdot}$ (dashed violet line), $WC^{\beta}$-$WC^{\alpha}$(on the $O^{\cdot}$ atom) (dotted violet line) distances. Lower panel: The spread functional of the moving electron. Vertical green line shows the point in which the proton is midway between the oxygen atoms.

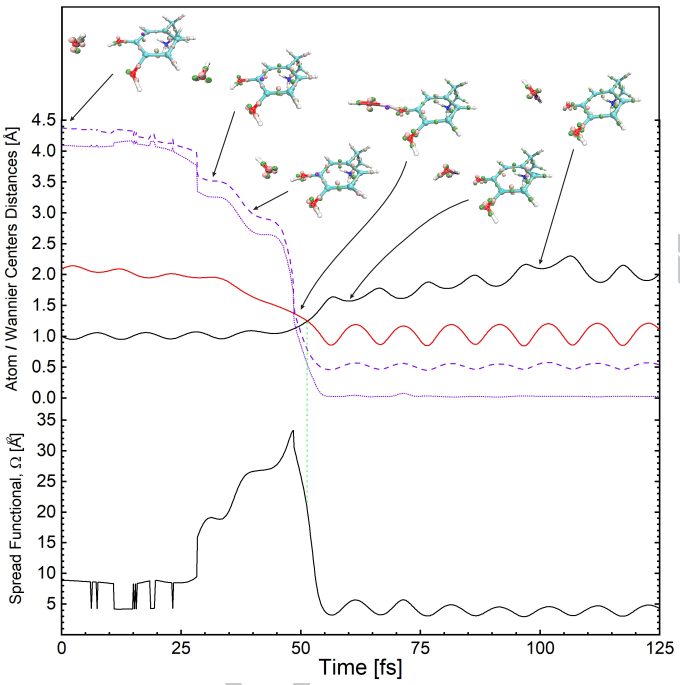


A typical example of a dehydrogenation via PCET mechanism is presented in Fig. 2. The reaction starts approximately 30 fs after the beginning of the simuation. H1 proton and electron (loosely represented as a Wannier centroid (WC)) are simultaneously removed and within 30 fs the reaction is completed. The spread functional indicates that electron density is not localized from 30 to 60 ps, i.e. the electron transfer ocurrs. The fluctuations of the spread functional in the beginning of the simulation are due to the difficulties related to the localization of Wannier orbitals in the aromatic systems [36].

Fig. 3 depicts a representative simulation which occurs via MS-PCET mechanism. Again, an electron is transferred directly from the aromatic ring towards the hydroxyl radical avoiding water molecules, which results in the formation of a hydroxyl ion. Subsequently, there is a proton transfer via two water molecules to the hydroxyl ion in a Grotthuss-like mechanism. Evident collapse of the spread functional along the reaction path shows that the electron is being transferred in $\approx$ 75 fs. This is somewhat longer time than in the case of the PCET mechanism since the hydroxyl radical is further away from the dopamine. We also note that the electron transfer starts in the first few femtoseconds of the simulation. In our simulations, different number of water molecules participated in proton transfer, being in range from one to five.

### 3.2. *Peroxyl and methoxy radicals*

Although peroxyl and methoxy radicals are significantly less reactive than hydroxyl radical, we observed that their reactions with dopamine also lasted less than one picosecond. The exception was one simulation with the peroxyl radical, which we found to be nonreactive. For both radicals, HAT mechanism competes with PCET mechanism: 3 out of 4 for methoxy and 2 out of 3 for peroxyl radical. The representative HAT reaction mechanism for methoxy radical is presented on Fig. 4. In this example, the radical is in the vicinity of the O1-H1 catechol group. The reaction is characterized with the simultaneous transfer of H1 proton and electron originating from the O1-H1 bond. Another electron ($WC_1^{\beta}$) is then afterwards transferred from the C1-C2 to the O1-H1 bond to compensate the loss of the $\sigma$ electron density ($WC_2^{\beta}$). Changes of spread functional values illustrates motion of both electrons. This finding shows that the hydrogen atom transfer always ends up with the loss of electron density from the aromatic moiety. Beside newly discovered HAT mechanism, for both radicals we observed in few cases MS-PCET mechanism, being of the similar characteristics compared to MS-PCET of hydroxyl radical.

### 3.3. *The origin of the BLYP functional failure to account the reaction barriers*

To summarize the previous section, the main findings of the BLYP-based molecular dynamics simulations are: the electron transfer from dopamine to free radicals occurs immediately after the simulations begins. It triggers a proton transfer to the radical or water molecule, depending on which molecule is more available to receive a proton. Irrespective of the free radical, the formal hydrogen transfer proceeds without a barrier and it is finished in less than a picosecond. These findings are opposite to the available experimental results [7]. The rate constant for dopamine scavenging for hydroxyl radical is $5.9\times10^{9}$ $M^{-1}$ $s^{-1}$ at pH 4.7 [3], those for peroxyl and methoxy radicals are certainly several orders of magnitude smaller [13, 14]. According to the transition state theory, this rate corresponds to a free energy barrier of 17.2 kJ/mol. Thus, the BLYP functional significantly underestimates the free energy barrier for a formal hydrogen atom transfer. In order to test the ability of the BLYP functional to properly describe hydrogen transfer reaction, we performed static quantum-chemical calculations in order to locate the transition state for the reaction between dopamine and

hydroxyl radical in the gas phase. Its optimization is essential for the estimation of the barrier height for the analyzed reaction. Unfortunately, we did not succeed in the location of this transition state, which is another indication that the BLYP functional has difficulties to describe this system. On the other hand, the M06-2X functional is known to be reliable for processes that involve organic radicals [37]. The energy barrier computed as a difference in electronic energies between the transition state and pre-reaction hydrogen bonded complex amounts to 32 kJ/mol at M06-2X/6-31+G(d,p) level computed with Gaussian program package [38].

There are two deficiencies of the BLYP functional which might lead to this failure: inability to account a multireference character of the transition state for hydrogen atom transfer between hydroxyl group and a radical [39, 40] and the self-interaction error [41, 42]. The first deficiency in not decisive since its magnitude is 4-8 kJ/mol in the gas phase and it is even reduced by solvation [40]. The second weakness is related to a property of the BLYP functional to delocalize charge and spin densities in systems with an odd number of electrons. In our case, an electron in the highest occupied molecular orbital will split between dopamine, radical and water molecules to decrease its own self-interaction. Fig. S1 in the SI displays Hirshfeld charges and spins of dopamine, hydroxyl radical and a water molecule hemibonded to the hydroxyl radical sampled in the first 24 fs from the simulation presented in Figure 2. Although the dopamine and hydroxyl radical should have the charges equal to one and zero, respectively, in this particular simulation their values before the reaction are approximately -0.17 and 0.87 a.u. Furthermore the unpaired electron on the hydroxyl radical is also delocalized to a nearby water molecule. The self-interaction error lowers the energy gap between the ground and excited state, which faciliates the electron transfer between the dopamine and hydroxyl radical. Thus, we believe that the self-interaction error is a major cause of the ultrafast reaction between the dopamine and free radicals. In order to support this explanation, we performed a one picosecond long simulation in which we applied the self-interaction correction to the unpaired electron [41]. This correction scales the Hartree and exchange-correlation energies by empirical parameters. We applied the same values of the parameters as recommended by VandeVondele and Sprik [41]. The correction forces the unpaired electron to reside on the hydroxyl radical (see Fig. S2 in the SI). As a consequence, there was no reaction between dopamine and hydroxyl radical within one picosecond. In addition, the BLYP+D3+SIC potential energy barrier for a hydrogen atom transfer in gas phase between dopamine and hydroxyl radical is calculated to be 54 kJ/mol. This is in line with the explanation that the self-interaction error is responsible for the failure of the BLYP functional to correctly describe the reaction barriers between the dopamine and free radicals. We also report that computational demanding for the inclusion of the self-interaction correction in the simulation is considerably high. Thus, by taking into account the self-interaction correction, it might not be possible to spontaneously observe the reaction in the simulation in a reasonable computational time but enhanced sampling techniques would be necessary. The work on this issue is in progress.

## 4. Conclusions

In this work, we carried out a first principle molecular dynamics study of the reactivity of the dopamine towards hydroxyl, peroxyl and methoxy radicals in aqueous medium. The goal of this work was to find the most probable mechanisms for these reactions. The simulations were performed by using density functional theory and the BLYP functional since more advanced functionals were far too computationally demanding. In the case when radicals were not in the vicinity of dopamine's hydroxyl groups, all radicals reacted with dopamine via MS-PCET mechanism. Otherwise, hydroxyl radical reacted via PCET, whereas peroxyl and methoxy radical exhibit both HAT and PCET mechanisms. The hydrogen atom transfer always ends up with the loss of electron density of the aromatic $\pi$ orbital. The equal timescales of all reactions indicated that the BLYP functional underestimates free energy barriers for these processes. Nevertheless, the reported mechanisms are not incorrect. The origin of the BLYP functional to improperly address the reaction barriers was attributed to the self-interaction error. By applying the correction for this error, we demonstrated that the radical reactions do not proceed on the femtosecond timescale.

## 5. Acknowledgement

M. B., P. M. and E. M. acknowledge the Ministry of Education, Science, and Technological Development of the Republic of Serbia for the financial support (Contract No. 172040).

## References

[1] K. J. Barnham, C. L. Masters, A. I. Bush, Neurodegenerative Diseases and Oxidative Stress, Nat. Rev. Drug Discov. 3 (2004) 205–214.
[2] H. Sies, Oxidative Stress: Oxidants and Antioxidants, Exp. Physiol. 82 (1997) 291–295.
[3] H. W. Richter, W. H. Waddell, Mechanism of the Oxidation of Dopamine by the Hydroxyl Radical in Aqueous Solution, J. Am. Chem. Soc. 105 (1983) 5434–5440.
[4] T. Kawashima, K. Ohkubo, S. Fukuzumi, Radical Scavenging Reactivity of Catecholamine Neurotransmitters and the Inhibition Effect for DNA Cleavage, J. Phys. Chem. B 114 (2010) 675–680.
[5] K. Jodko-Piórecka, G. Litwinienko, Antioxidant Activity of Dopamine and L-DOPA in Lipid Micelles and Their Cooperation With an Analogue of $\alpha$-Tocopherol, Free Radic. Biol. Med. 83 (2015) 1–11.
[6] D. Dimić, D. Milenković, J. D. Marković, Z. Marković, Thermodynamic and Kinetic Analysis of the Reaction Between Biological Catecholamines and Chlorinated Methylperoxy Radicals, Mol. Phys. 116 (2017) 1166–1178.
[7] C. Iuga, J. R. Alvarez-Idaboy, A. Vivier-Bunge, ROS Initiated Oxidation of Dopamine Under Oxidative Stress Conditions in Aqueous and Lipidic Environments, J. Phys. Chem. B 115 (2017) 12234–12246.
[8] R. Álvarez Diduk, A. Galano, Adrenaline and Noradrenaline: Protectors Against Oxidative Stress or Molecular Targets?, J. Phys. Chem. B 119 (2015) 3479–3491.
[9] A. Galano, Free Radicals Induced Oxidative Stress at a Molecular Level: the Current Status, Challenges and Perspectives of Computational Chemistry Based Protocols, J. Mex. Chem. Soc. 59 (2015) 231–262.

[10] K. Mukai, K. Nagai, Y. Egawa, A. Ouchi, S. Nagaoka, Kinetic Study of Aroxyl-Radical-Scavenging and $\alpha$-Tocopherol-Regeneration Rates of Five Catecholamines in Solution: Synergistic Effect of $\alpha$-Tocopherol and Catecholamines, J. Phys. Chem. B 120 (2016) 7088–7097.

[11] J. Quintero-Saumeth, D. A. Rincón, M. Doerr, M. C. Daza, Concerted Double Proton-Transfer Electron-Transfer Between Catechol and Superoxide Radical Anion, Phys. Chem. Chem. Phys. 19 (2017) 26179–26190.

[12] D. Dimić, D. Milenković, J. D. Marković, Z. Marković, Antiradical Activity of Catecholamines and Metabolites of Dopamine: Theoretical and Experimental Study, Phys. Chem. Chem. Phys. 19 (2017) 12970–12980.

[13] M. Petković, D. Nakarada, M. Etinski, When Hydroquinone Meets Methoxy Radical: Hydrogen Abstraction Reaction from the Viewpoint of Interacting Quantum Atoms, J. Comput. Chem. 39 (2018) 1868–1877.

[14] D. Nakarada, M. Petković, Mechanistic Insights on How Hydroquinone Disarms OH and OOH Radicals, Int. J. Quantum Chem. 118 (2018) e25496.

[15] D. Dimić, D. Milenković, J. Ilić, B. Šmit, A. Amić, Z. Marković, J. Dimitrić-Marković, Experimental and Theoretical Elucidation of Structural and Antioxidant Properties of Vanillylmandelic Acid and its Carboxylate Anion, Spectrochim. Acta A 198 (2018) 61–70.

[16] C. J. Mundy, M. E. Colvin, A. A. Quong, Irradiated Guanine: A Car-Parrinello Molecular Dynamics Study of Dehydrogenation in the Presence of an OH Radical, J. Phys. Chem. A 106 (2002) 10063–10071.

[17] Y. Wu, C. J. Mundy, M. E. Colvin, R. Car, On the Mechanisms of OH Radical Induced DNA-Base Damage: A Comparative Quantum Chemical and Car-Parrinello Molecular Dynamics Study, J. Phys. Chem. A 108 (2004) 2922–2929.

[18] J. R. Asher, N. L. Doltsinis, M. Kaupp, Ab Initio Molecular Dynamics Simulations and g-Tensor Calculations of Aqueous Benzosemiquinone Radical Anion: Effects of Regular and "T-Stacked" Hydrogen Bonds, J. Am. Chem. Soc. 126 (2004) 9854–9861.

[19] P. Vassilev, M. J.Louwerse, E. J. Baerends, Ab Initio Molecular Dynamics Simulation of the OH Radical in Liquid Water, Chem. Phys. Lett. 398 (2004) 212–216.

[20] F. Constanzo, M. Sulpizi, J. VandeVondele, R. G. D. Valle, M. Sprik, Ab Initio Molecular Dynamics Study of Ascorbic Acid in Aqueous Solution, Mol. Phys. 105 (2007) 17–23.

[21] J. R. Asher, M. Kaupp, Car-Parrinello Molecular Dynamics Simulations and EPR Property Calculations on Aqueous Ubisemiquinone Radical Anion, Theor Chem Account 119 (2008) 477.

[22] R. N. Barnett, J. Joseph, U. Landman, G. B. Schuster, Oxidative Thymine Mutation in DNA: Water-Wire-Mediated Proton-Coupled Electron Transfer, J. Am. Chem. Soc. 135 (2013) 3904–3914.

[23] L. Lespade, Ab initio Molecular Dynamics of the Reaction of Quercetin with Superoxide Radical, Chem. Phys. 475 (2016) 32–38.

[24] L. Lespade, Ab initio Molecular Dynamics of the Reactivity of Vitamin C toward Hydroxyl and $HO_2/O_2$ Radicals, J. Mol. Model (2017) 23:347 23 (2017) 347.

[25] L. Lespade, Ab initio Molecular Dynamics of Electron Transfer from Gallic Acid to Small Radicals: A Comparative Study Between Hydroxyl and Nitrogen Dioxide Radicals, Comput. Theor. Chem. 1135 (2018) 6–10.

[26] J. VandeVondele, M. Krack, F. Mohamed, M. Parrinello, T. Chassaing, J. Hutter, QUICKSTEP: Fast and Accurate Density Functional Calculations Using a Mixed Gaussian and Plane Waves Approach, Comput. Phys. Commun. 167 (2005) 103–128.

[27] A. D. Becke, Density-Functional Exchange-Energy Approximation with Correct Asymptotic-Behavior, Phys. Rev. A 38 (1988) 3098–3100.

[28] C. T. Lee, W. T. Yang, R. G. Parr, Development of the Coll-Salvetti Correlation-Energy Formula into a Functional of the Electron-Density, Phys. Rev. B 37 (1988) 785–789.

[29] S. Grimme, J. Antony, S. Ehrlich, H. Krieg, A Consistent and Accurate Ab Initio Parametrization of Density Functional Dispersion Correction (DFT-D) for the 94 Elements H-Pu, J. Chem. Phys. 132 (2010) 154104.

[30] S. Goedecker, M. Teter, J. Hutter, Separable Dual-Space Gaussian Pseudopotentials, Phys. Rev. B 54 (1996) 1703–1710.

[31] G. Lippert, J. Hutter, M. Parrinello, A Hybrid Gaussian and Plane Wave Density Functional Scheme, Mol. Phys. 92 (1997) 477–487.

[32] G. Bussi, D. Donadio, M. Parrinello, Canonical Sampling Through Velocity Rescaling, J. Chem. Phys. 126 (2007) 014101.

[33] M. Brehm, B. Kirchner, TRAVIS - A Free Analyzer and Visualizer for Monte Carlo and Molecular Dynamics Trajectories, J. Chem. Inf. Model. 51 (2011) 2007–2023.

[34] M. M. Ristić, M. Petković, B. Milovanović, J. Belić, M. Etinski, New Hybrid Cluster-Continuum Model for pKa Values Calculations: Case Study of Neurotransmitters Amino Group Acidity, Chem. Phys. 516 (2019) 55–62.

[35] E. García-Hernández, J. Garza, Reactivity Sites in Dopamine Depend on its Intramolecular Hydrogen Bond, J. Mex. Chem. Soc. 61 (2017) 222–228.

[36] M. Thomas, M. Brehm, B. Kirchner, Voronoi Dipole Moments for the Simulation of Bulk Phase Vibrational Spectra, Phys. Chem. Chem. Phys. 17 (2015) 3207–3213.

[37] Y. Zhao, D. G. Truhlar, How Well Can New-Generation Density Functionals Describe the Energetics of Bond-Dissociation Reactions Producing Radicals?, J. Phys. Chem. A 112 (2008) 1095–1099.

[38] M. J. Frisch, G. W. Trucks, H. B. Schlegel, G. E. Scuseria, M. A. Robb, J. R. Cheeseman, G. Scalmani, V. Barone, B. Mennucci, G. A. Petersson, H. Nakatsuji, M. Caricato, X. Li, H. P. Hratchian, A. F. Izmaylov, J. Bloino, G. Zheng, J. L. Sonnenberg, M. Hada, M. Ehara, K. Toyota, R. Fukuda, J. Hasegawa, M. Ishida, T. Nakajima, Y. Honda, O. Kitao, H. Nakai, T. Vreven, J. A. Montgomery, Jr., J. E. Peralta, F. Ogliaro, M. Bearpark, J. J. Heyd, E. Brothers, K. N. Kudin, V. N. Staroverov, T. Keith, R. Kobayashi, J. Normand, K. Raghavachari, A. Rendell, J. C. Burant, S. S. Iyengar, J. Tomasi, M. Cossi, N. Rega, J. M. Millam, M. Klene, J. E. Knox, J. B. Cross, V. Bakken, C. Adamo, J. Jaramillo, R. Gomperts, R. E. Stratmann, O. Yazyev, A. J. Austin, R. Cammi, C. Pomelli, J. W. Ochterski, R. L. Martin, K. Morokuma, V. G. Zakrzewski, G. A. Voth, P. Salvador, J. J. Dannenberg, S. Dapprich, A. D. Daniels, O. Farkas, J. B. Foresman, J. V. Ortiz, J. Cioslowski, D. J. Fox, Gaussian 09 Revision D.01, gaussian Inc. Wallingford CT 2009.

[39] O. Tishchenko, D. G. Truhlar, Benchmark Ab Initio Calculations of the Barrier Height and Transition-State Geometry for Hydrogen Abstraction from a Phenolic Antioxidant by a Peroxy Radical and Its Use to Assess the Performance of Density Functionals, J. Phys. Chem. Lett. 3 (2012) 2834–2839.

[40] A. Galano, L. Muñoz-Rugeles, J. R. Alvarez-Idaboy, J. L. Bao, D. G. Truhlar, Hydrogen Abstraction Reactions From Phenolic Compounds by Peroxyl Radicals: Multireference Character and Density Functional Theory Rate Constants, J. Phys. Chem. B 120 (2015) 4634–4642.

[41] J. VandeVondele, M. Sprik, A Molecular Dynamics Study of the Hydroxyl Radical in Solution Applying Self-Interaction-Corrected Density Functional Methods, Phys. Chem. Chem. Phys. 7 (2005) 1363–1367.

[42] P. H.-L. Sit, M. Cococcioni, N. Marzari, Realistic Quantitative Descriptions of Electron Transfer Reactions: Diabatic Free-Energy Surfaces from First-Principles Molecular Dynamics, Phys. Rev. Lett. 97 (2006) 028303.

Figure 3: Upper panel: Insets with configurations during MS-PCET reaction of dopamine with hydroxyl radical. Other water molecules were omitted for clarity. The WCs are depicted by pink ("$\alpha$" spin - WC$^{\alpha}$) and green ("$\beta$" spin - WC$^{\beta}$) spheres, whereas violet sphere represent WC$^{\beta}$ of moving electron. Middle panel: Evolution of WC$^{\beta}$-O$^{\cdot}$ (dashed violet line), WC$^{\beta}$-WC$^{\alpha}$(on the O$^{\cdot}$ atom) (dotted violet line), O1-H1 (black line), H1-O$^{w1}$ (dashed blue line), O$^{w1}$-H$^{w1}$ (dashed light blue line), H$^{w1}$-O$^{w2}$ (light blue line), O$^{w2}$-H$^{w2}$ (blue line), H$^{w2}$-O$^{\cdot}$ (red line) distances. Lower panel: The spread functional of the moving electron. Vertical green lines show points in which the proton is midway between the oxygen atoms.

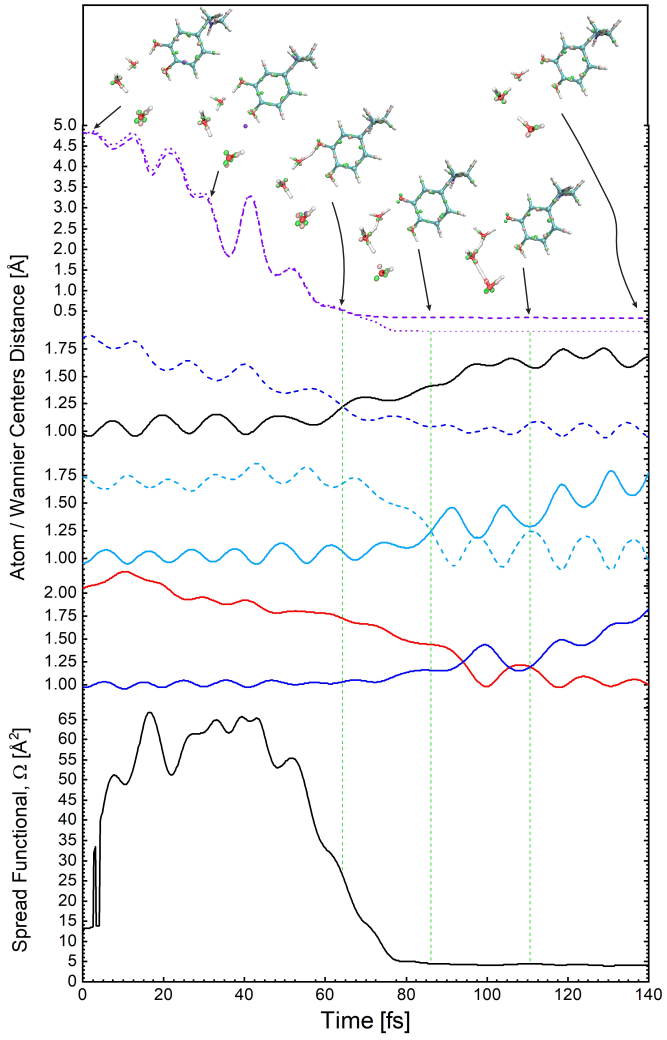


Figure 4: Upper panel: Insets with configurations during HAT reaction of dopamine with methoxy radical. Other water molecules were omitted for clarity. The WCs are depicted by pink ("$\alpha$" spin - WC$^{\alpha}$) and green ("$\beta$" spin - WC$^{\beta}$) spheres, whereas violet sphere represent WC$^{\beta}$ of moving electrons. Middle panels: Evolution of O1-H1 (black line), H1-O$^{\cdot}$ (red line), WC$^{\beta}_{1}$-O1 (violet line), WC$^{\beta}_{2}$-O$^{\cdot}$ (dashed violet line), WC$^{\beta}$-WC$^{\alpha}$ (dotted violet line) distances. Lower panel: The spread functional of the moving electrons $\beta_1$ (dashed black line) and $\beta_2$ (black line). Vertical green line shows the point in which the proton is midway between the oxygen atoms.

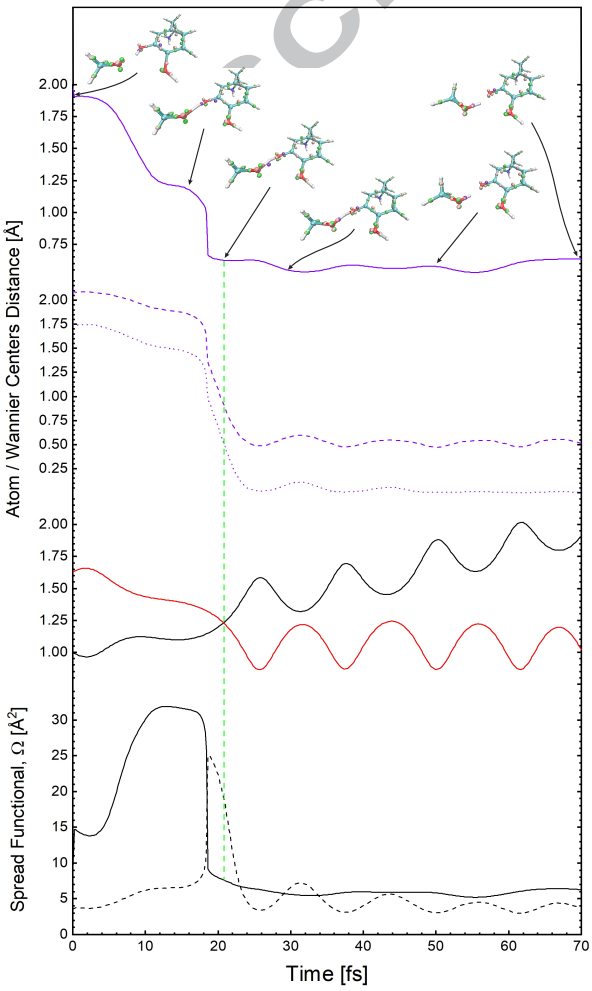

- The formal hydrogen transfer from dopamine to free radicals does not involve stable intermediates.
- The electron transfer results in a loss of electron density from the aromatic π orbital.
- The self-interaction error is responsible for underestimation of the reaction timescales.
- The self-interaction correction to the BLYP functional provides a similar reaction barrier as more advanced M06-2X functional.